Dyeing to See: Using Microscopy to Assess the Impact of the Nucleic Acid Dye DAPI on the Chemotactic Behavior of Soil-Dwelling Bacteria

J. Amanda Toepfer
University of Virginia
Department of Chemical Engineering
BIOL 507, Final Project

Chemotactic bacteria have the potential to play an important role in the remediation of contaminated groundwater at the field scale. In order to determine the impact of chemical gradients on the transport of bacteria, a method to visualize the bacteria of interest must be implemented. Previous field-scale transport studies have utilized the nucleic acid dye, 4',6-diamidino-2-phenylindol (DAPI), as a primary means of bacteria detection. This paper explores microscopic methods to determine differences in the chemotactic behavior of *Pseudomonas putida* F1 stained and unstained with DAPI in response to the attractant acetate. There is evidence that suggests staining with DAPI impairs *P. putida* F1's response to acetate, thereby altering the transport properties of the bacteria. Altered response in the presence of DAPI could have significant ramifications on the methods used to visualize microbial transport in past and future field studies.

Introduction

Groundwater contamination is a problem endemic to much of the world. In the United States, the causes of contamination are numerous and include sewage, gasoline, and detergents. Technology compounds the problem: innovative new chemicals or byproducts of production processes have proven to be toxic in some significant cases over the past 30 years. Disposal of these chemicals before more stringent regulations were established was often directly into water or land areas where they could leech into the groundwater. Particularly problematic chemicals include trichloroethylene (TCE), a chemical produced from cleaning solvents and dry cleaning; polychlorinated biphenyls (PCBs), chemicals that were used in plasticizers and heat exchanger fluids as well as being used as insulators; and 2, 4, 6-trinitrotoluene (TNT), a common military explosive. These chemicals especially pose a risk due to their tendency for environmental longevity (Iwamoto and Nasu, 2001).

One proven method of remediating contaminated groundwater and soil is through microbial consumption of the contaminant, or bioremediation. The United States Geological Survey (USGS) conclusively demonstrated bioremediation in the aftermath of a jet fuel spill in Hanahan, South Carolina (USGS Fact Sheet 054-95). The USGS is also currently monitoring the natural attenuation of a contaminant plume from Otis Air Base on Cape Cod, MA. This area is of particular interest, as their monitoring efforts both characterized the plume and made the entire region ideal for site-testing. The first report of the contaminant plume indicated it was 3000 ft wide, 75 ft thick, and 11,000 ft long, and was studied as part of a national survey to determine the fate of toxic wastes in groundwater. The plume was caused by discharge of secondarily treated sewage into the surrounding aquifer (OFR 84-475). As a result of their characterization, the plume and surrounding areas have been the site of field-tests for microbial and colloidal transport.

Harvey, et al (1989), first explored transport of DAPI-stained indigenous bacteria through Cape Cod aquifer and found the bacteria could be transported across the aquifer. Scholl and Harvey (1992) found that transport and sorption properties of DAPI-stained indigenous bacteria differed in the contaminated and uncontaminated regions of Cape Cod, MA. They found that there was less bacterial sediment attachment in the presence of dissolved organic material (DOM). High levels of DOM are an indication of contamination. Becker, et al (2003) explored transport of stained bacteria and microspheres in crystalline bedrock. They found that bacteria were likely to be heavily filtered in fractured rock, and attributed late breakthrough of motile bacteria to their ability to explore stagnant regions and pore spaces that non-motile bacteria and colloids could not reach. Many authors showed transport of bacteria is possible through the Cape Cod aquifer, but none explicitly explored effects of chemical gradients on bacterial breakthrough curves at the field scale.

Chemotaxis is the term used to describe the biased movement of bacteria in response to a chemical gradient. Implementation of chemotactically inclined bacteria in remediation efforts may facilitate contaminant degradation in the aquifer. There is evidence to support that chemotactic bacteria are more efficient at

degrading contaminants than their non-chemotactic or non-motile counterparts. For example, Law and Aitken (2003) saw significant naphthalene degradation in non-aqueous environments with chemotactic bacteria versus non-chemotactic or non-motile bacteria. Chemotaxis has the added benefit of greater accessibility to contaminants. Using Becker, et al (2003) as an example, should the stagnant regions in crystalline bedrock described in the paper contain a carbon source, they may be more efficiently explored by chemotactic bacteria. These regions would be less likely to be reached by bacteria unable to direct their paths toward a potential attractant. Analogous applications would be transport into tight pore spaces in fine-sand aquifers and clay lenses. Sherwood, et al (2003) cites that many bacteria are able to swim at speeds faster than that of most groundwater, and argues that random motility effects might not be negligible compared to advection. Consequently, if random motility is not negligible, biased motility could have a large impact on remediation efforts, especially during bioaugmentation.

Our laboratory currently works with *Pseudomonas putida* F1, a toluene-degrading, rod-shaped bacterium native to soil and groundwater environments. Our aim is to show that some *Pseudomonades* are impacted by chemical gradients not only at porous media interfaces on the microscopic scale (e.g., Kusy, 2005), but that this translates to a visible effect on the macroscopic scale. In order to explore this, we must choose a method of visualization. A number of important USGS studies over the past 15 years have utilized DAPI as a primary method of visualization (e.g., Harvey, et al, 1989; Scholl and Harvey, 1992; Becker, et al, 2003). DAPI is a nucleic acid dye with an excitation wavelength of 358 nm and a maximum emission wavelength of 461 nm. The goal of this study is to determine what microscopic methods are best to qualitatively and quantitatively assess the impact of DAPI on the chemotactic ability of *P. putida* F1. Assessing the impact of the visualization method is important for determining the experimental method for field study

Materials and Methods

Agarose Plug Assays

Bacterial Preparation

P. putida F1 was grown in 50 mL of Luria Broth (10 g/L Tryptone, Difco, Sparks, MD; 5 g/L Yeast Extract, Difco, Sparks, MD; 10 g/L NaCl, FisherScientific, Fair Lawn, NJ) and 1mM sodium acetate (FisherScientific, Fair Lawn, NJ) in 250 mL shaker flasks at 160 rpm and 27.2ºC. Solutions were allowed to grow until they reached an optical density at 590nm (OD_{590}) of ~1.0, and were then filtered through 0.22 μm Nucleopore filters and resuspended in 10% random motility buffer (RMB, 11.2 g/L K_2HPO_4, 4.8 g/L KH_2PO_4, 0.029g/L EDTA, all FisherScientific, Fair Lawn, NJ) and brought to an OD_{590} of ~1. Control samples (those without stain) were left as-is. DAPI-stained samples were stained in a one-to-one mixture of bacteria in 10% RMB and 100 mg/L DAPI (Molecular Probes #D1306, Eugene, OR) for 20 minutes at 160 rpm and 27.2ºC. Stained samples were shielded from light before, during, and after staining. The DAPI-bacteria suspension was then filtered and resuspended in 10% RMB and brought to an OD_{590} of ~1. Solution containers were wrapped with tin-foil to prevent extraneous light.

Plug Assay

Agarose plug assays were performed between February and August 2005. The protocol was developed based on Parales, et al (2000), and via personal communication with Mira Olson (UVA, Charlottesville, VA). Briefly, a 2% agarose (low melting, NuSieve GTG Agarose, FMC Bioproducts, Rockland, MN) plug in 10% RMB containing varying amounts of the attractant acetate was heated to 70ºC until completely melted. A drop (10μL) of the molten agarose was placed in the center of a clean glass microscope slide, and a chamber was created with two cover slips on either side of the plug and an additional cover slip on top of the plug. A bacterial suspension (OD_{590} of ~1.0) +/- DAPI was pipetted into the chamber slowly to avoid convective effects, and the accumulation pattern of the bacteria was observed via microscope over time.

Microscopic Methods

Stereomicroscopy

Human eyes together with the brain form stereoscopic images by fusing together the two separate images formed on each retina. The image from one eye is taken from a viewpoint a few degrees different than on the other eye. A stereomicroscope mimics this ability and transmits two images that differ by 10-12 degrees to create an image with depth (Nikon, "Introduction to Stereomicroscopy). A Zeiss Stemi SV8 Stereomicroscope with 0.8x zoom

was used in the stereomicroscopy portion of the experiment. Dual-arm fiber optic illuminators (Schott, KL-1500) were used at a 45° angle incident to the microscope slide to simulate dark-field light scattering. Images were captured with a Dage-MTI (Michigan City, IN) CCD camera using *QuickImage* software. Analysis was performed using ImageJ (National Institute of Health).

Widefield Microscopy

Traditional brightfield microscopy uses scattered light to illuminate an image. Phase contrast microscopy produces high contrast images of transparent specimens by using an optical mechanism to translate changes in phase to changes in amplitude. The result is visualized as changes in contrast. (Nikon, "Phase Contrast Microscopy") For this study, typical brightfield microscopy was merged with phase contrast to simulate dark-field light scattering but is not true dark-field microscopy). A phase-3 condenser phase annulus was placed in the wide-field microscope's optical path (figure 1). The light emerging from the condenser annulus is often thought of as a hollow cone of light with a dark center. In this set-up, the light hit the specimen at approximately 45°. This angle of incident was similar to the fiber optic light set-up with the stereomicroscopy and allowed maximum contrast between the agarose plug and the surrounding solution. Two microscope systems were used: 1) Olympus (IX-70) Infinity corrected inverted microscope with a 4x Plan Achromat objective (N.A. 0.10, 22mm working distance) using a Hamamatsu Orca-2 CCD camera, and 2) Zeiss Axiostar upright microscope with a 3.2x objective (N.A. 0.07, 160mm tube length) and 3x magnification using a Dage-MTI (Michigan City, IN) CCD camera and *QuickImage* software.

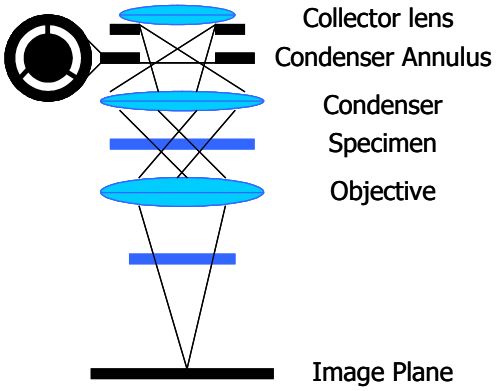

Figure 1: Optical path used in the widefield microscopy systems. In each system, the light from the illumination source passes through the collector lens and then passes through a condenser annulus, as in phase microscopy. The angled light hits the specimen, passes through the objective and then is formed on the image plane. Unlike in true phase microscopy, there is no phase ring within the objective; the resulting image is more akin to dark field light scattering.

Results and Discussion

Widefield Zeiss System

Control (– DAPI)

Figure 2 shows two images captured using the Zeiss widefield system. In both the 0M acetate plug and the 0.1M acetate plug, peaks are evident at 9 minutes. This is likely due to the motility of the bacteria—highly motile bacteria

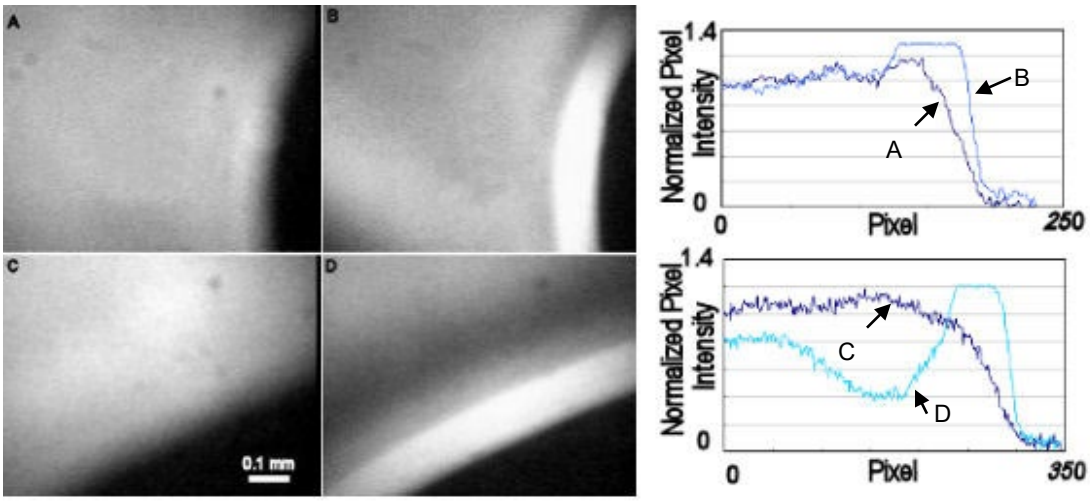

Figure 2: These images show the chemotactic ability of unstained *P. putida* F1 to acetate. A and B are time captured images of a 0 M acetate plug surrounded by unstained *P. putida* at times of 0 minutes and 9 minutes, respectively. C and D are time captured images of a 0.1 M acetate plug surrounded by unstained *P. putida* at times of 0 and 9 minutes respectively. The plots to the right show the intensity profiles of the indicated images. Chemotaxis is seen in the plots as a trough followed by a peak in the plots. The trough is readily visible in the 0.1M, t=9 minutes plot, and peaks are visible in both 0M and 0.1M plots at t=9 minutes.

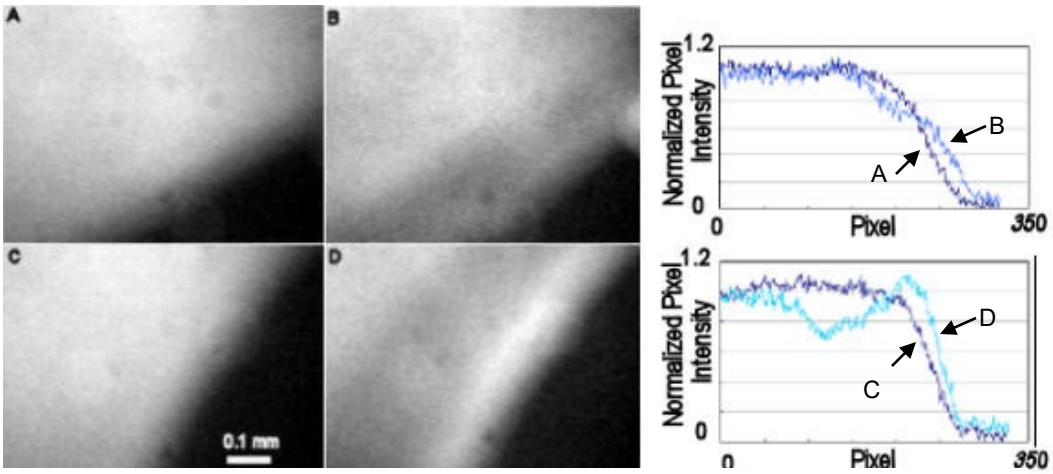

Figure 3: These images show the chemotactic ability of DAPI-stained *P. putida* F1 to acetate. A and B are time captured images of a 0 M acetate plug surrounded by DAPI-stained *P. putida* at times of 0 minutes and 9 minutes, respectively. C and D are time captured images of a 0.1 M acetate plug surrounded by DAPI-stained *P. putida* at times of 0 and 9 minutes respectively. The plots to the right show the indicated intensity profiles. Chemotaxis is seen in the plots as a trough followed by a peak in the plots. A small trough and peak are visible in the 0.1M, t=9 minutes plot. No peak is visible in the 0M plot at t=9 minutes.

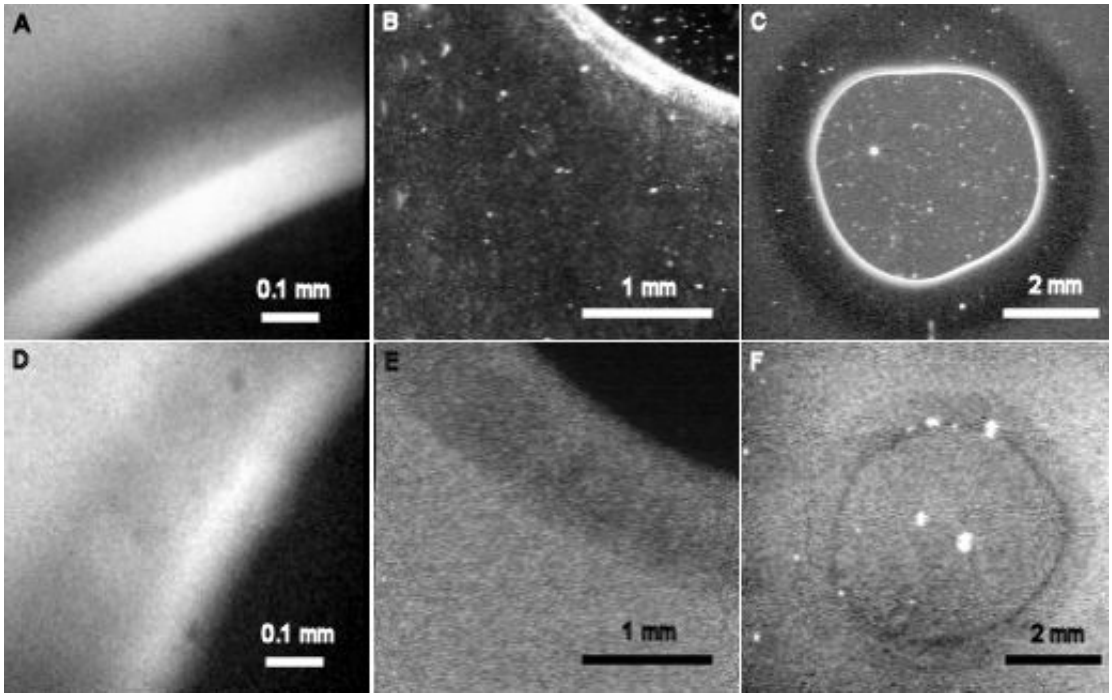

Figure 4: This figure compares chemotactic response of stained and unstained bacteria to a plug concentration of 0.1M for 3 different microscopy systems. A) This image is *P. putida* F1 with no DAPI imaged on the Zeiss system with a 3.2x objective and 3x zoom at time = 9 minutes using light scattering. Chemotaxis is apparent, although the plug interface is at saturation. The outer limits of response are undetectable. B) This image is *P. putida* F1 with no DAPI imaged on the Olympus wide-field system at the Keck Center for Cellular Imaging (KCCI) with a 4x objective at time = 9 minutes using light scattering. Chemotaxis is apparent, but the frame barely extends to the outer limits of response, and artifacts from the coverslips and agarose are visible. D) This image is *P. putida* F1 with no DAPI imaged on the Zeiss stereomicroscope using light scattering. The full range of chemotaxis is visible, but as in image B, artifacts from the coverslips and agarose are visible. D) This image is *P. putida* F1 with DAPI imaged on the Zeiss system with a 3.2x objective and 3x zoom at time = 9 minutes using light scattering. Chemotaxis is apparent, although the plug interface is at saturation. The response in the presence of the nucleic acid is small enough that this level of magnification is warranted. E) This image is *P. putida* F1 with DAPI imaged on the Olympus wide-field system at KCCI with a 4x objective at time = 9 minutes. The image was taken via DAPI excitation, and as a result, artifacts like those seen in image B are not visible. Slight chemotaxis is visible. F) This image is *P. putida* F1 with DAPI imaged on the Zeiss stereomicroscope using light scattering. Chemotaxis appears to be less evident, likely warranting the use of increased magnification as in D and E.

tend to get stuck at the interface of the plug and the free solution. This is not a true chemotactic response, although an accumulation is seen, as in figure 2B. A true chemotactic response shows a void area where the bacteria population has evacuated and migrated to the source of the attractant. This is why we look for a characteristic trough, as in the plot for figure 2D, to indicate the presence of chemotaxis. Images captured in this set show saturation at the peak; repeated studies with no saturation after 9 minutes at the plug-free solution interface might also show a distinguishable peak shape for chemotaxis.

Stained Sample (+ DAPI)

Figure 3 shows two images captured using the Zeiss widefield system. In the 0M plug, no peaks of any kind are visible after 9 minutes. This is one clear difference from the control sample and may indicate that cells are far less motile in the presence of DAPI. A peak and a trough are seen after 9 minutes in the plots from the 0.1M plug, clearly indicating the presence of chemotaxis. However, the level of response is significantly reduced compared to the control sample.

Microscope Comparison

Comparison of Widefield Systems with Stereomicroscope Systems

Figure 4 shows 6 images comparing stained and unstained bacteria samples on three different microscope systems. The plug concentration in all images is 0.1M acetate, and thus chemotaxis should be evident in all images. Chemotaxis is evident in images 4 A and D, although for image A, it is unknown how far the response reaches. For bacteria that are known to have high chemotactic sensitivity, conducting experiments at this magnitude would severely undercut the expected level of response. For bacteria that have a low chemotactic sensitivity, however, this would be a good measure of total response.

Chemotaxis is again evident in image 4B, but again, the level of magnification makes it difficult to see how far the response reaches, as there is no area of the image containing an unaffected population. Slight chemotaxis is evident in image 4E. One advantage of image 4E is that it was taken via DAPI excitation, and as a result, artifacts from the microscope slide, coverslip and agarose plug are not seen. The images take on the Olympus system appear to be best for populations that elicit a medium level of chemotactic response.

Finally, the stereomicroscopic images of 4C and 4F show the largest-scale response the best. This system is best for images like that of 4C, as accumulation at the interface is seen, the void area is fully seen, and regions of bacteria outside the attractant gradient are also present. For bacteria populations with small responses, images like 4F do little to show an appreciable chemotactic response.

Conclusions

Microscopic methods to determine the response of *P. putida* to acetate were determined using two widefield systems and a stereomicroscope. It is evident that the choice of microscope depends upon the level of response of the bacterial population. A wide-field microscope is preferred for a smaller response, such as in the samples stained with DAPI. A stereomicroscope is preferred for a larger response, such as in the unstained sample. DAPI stained samples have the advantage of having fewer artifacts in the image, because when they are imaged with UV excitation, the artifacts from the glass and agarose do not excite. Overall, DAPI qualitatively reduces the response of *P. putida* F1 to acetate. This reduction changes the transport properties of the bacteria, and merits further quantitative investigation due to the implication of such a finding. On the whole, although all three microscopes are beneficial for viewing chemotaxis depending on the bacterial population, the stereomicroscope is the best for measuring a response that is most likely visible on the field scale.

Future Work

Additional work with this project includes quantitatively measure the chemotactic response of all samples. All of these microscopic methods show that while it is clear that the DAPI stained bacteria do respond to acetate, the level of response may depend on the amount of time the bacteria are stained. Samples in this study were stained for 20 minutes. It is possible that exploring additional staining times may show an optimal time to maximize chemotactic response in stained cells. Imaging the same conditions both with light scattering and DAPI excitation can show if differences in staining time also causes uneven population staining. That is, if there are differences in the two images, we can determine whether or not a viewed response is due solely to those bacteria that did not incorporate stain, as all bacteria will scatter light, but not all will fluoresce.

Additionally, it would be beneficial to test how DAPI affects the chemotactic ability of other bacterial strain. It would also be worth investigating how other nucleic acid dyes such as hydroethidine and Sybr Gold affect chemotaxis.

Acknowledgements

Funding for this work was provided by the National Science Foundation. Graduate Assistantships in Areas of National Need (GAANN) also provided the author additional funding support. Special thanks to the Keck Center for Cellular Imaging at the University of Virginia for the use of their facilities, and especially to Professors Ammasi Periasamy and Lance Davidson from the Biology department at the University of Virginia for all of their help learning about microscopy and the different systems available. Their help was invaluable to this project.

References

[1] Becker, Matthew, David W. Metge, Samantha A. Collins, Allen M. Shapiro, and Ronald W. Harvey. *Bacterial Transport Experiments in Fractured Crystalline Bedrock*. Ground Water, September-October 2003, Vol. 41, No. 5, 682-689.

[2] Harvey, Ronald W, Leah George, Richard L. Smith, and Denis R. LeBlanc. *Transport of Microspheres and Indigenous Bacteria through a Sandy Aquifer: Results of Natural- and Forced-Gradient Tracer Experiments*. Environmental Science and Technology, 1989, 23, 51-56.

[3] Harvey, Ronald W, and Hauke Harms. *Transport of Microorganisms in the Terrestrial Subsurface: In Situ and Laboratory Methods.* In Hurst, C.J., Knudsen, G.R., McInerney, M.J., Stetzenback, L.D., Crawford, R.L., eds., *Manual of Environmental Microbiology, 2nd Edition*, Washington, ASM Press, 2002, 753-776.

[4] Harwood, Caroline S., Kathy Fosnaugh, and Marilyn Dispensa. *Flagellation of Pseudomonas putida and Analysis of Its Motile Behavior*. Journal of Bacteriology, Vol. 171, No. 7, 1989, 4063-4066.

[5] Iwamoto, Tomotada, and Nasu, Masao. *Review: Current bioremediation practice and perspective*. Journal of Bioscience and Bioengineering, Vol 92, No 1, 1-8, 2001.

[6] Kusy, Kevin, PhD Thesis, 2005, Chemotaxis Mathematical Model.

[7] Law, Aaron M.J., and Michael D. Aitken. *Bacterial Chemotaxis to Naphthalene Desorbing from a Nonaqueous Liquid*. Applied and Environmental Microbiology, Vol. 69, 2003, 5968-5973.

[8] Nikon, "Introduction to Stereomicroscopy". MicroscopyU. http://www.microscopyu.com/articles/stereomicroscopy/stereointro.html

[9] Nikon, "Phase Contrast Microscopy". MicroscopyU. http://www.microscopyu.com/articles/phasecontrast/phasemicroscopy.html

[10] Parales, Rebecca E., Jayna L. Ditty, and Caroline S. Harwood. *Toluene-Degrading Bacteria Are Chemotactic towards the Environmental Pollutants Benzene, Toluene, and Trichloroethylene.* Applied and Environmental Microbiology, Sept 2000, 4098-4104.

[11] Scholl, Martha, and Ronald W. Harvey. Laboratory Investigations on the Role of Sediment Surface and Groundwater Chemistry in Transport of Bacteria through a Contaminated Sandy Aquifer. Environmental Science and Technology, Vol. 26, No. 7, 1992, 1410-1417.

[12] Sherwood, Juli L., James C. Sung, Roseanne M. Ford, Erik J. Fernandez, James E. Maneval, and James A. Smith. *Analysis of Bacterial Random Motility in a Porous Medium Using Magnetic Resonance Imaging and Immunomagnetic Labeling*. Environmental Science and Technology, 2003, 37, 781-785.

[13] U.S. Geological Survey Fact Sheet 054-95. *Bioremediation: Nature's Way to a Cleaner Environment*.

[14] U.S. Geological Survey Open-File Report 84-475. *Movement and Fate of Solutes in a Plume of Sewage Contaminated Ground Water, Cape Cod, Massachusetts: U.S. Geological Survey Toxic Waste Groundwater Contamination Program.* LeBlanc, D. 1984

[15] Yu, Wei, Walter K. Dodds, M. Katherine Banks, Jeannie Skalsky, and Eric A. Strauss. *Optimal Staining and Sample Storage Time for Direct Microscopic Enumeration of Total and Active Bacteria in Soil with Two Fluorescent Dyes*. Applied and Environmental Microbiology, Sept 1995, Vol. 61, No. 9, 3367-3372.